Formation of Ion Beams from Plasma Sources: Part I

J. Hyman Jr.,* W. O. Eckhardt,† R. C. Knechtli,‡ and C. R. Buckey§
Hughes Research Laboratories, Malibu, Calif.

The basic mechanisms involved in ion beam formation from plasma-type ion sources have been investigated. Theoretical concepts and their verification by experiments with an electron-bombardment ion source (hot-cathode Penning discharge) are described. The most important results can be summarized as follows: The conditions determining the position of the plasma boundary in an ion extraction system have been established quantitatively. It has been demonstrated that the plasma boundary can be simulated in an electrolytic tank, making this powerful tool applicable to the design of ion-optical systems for plasma-type sources. It has been shown that a careful electrode design is required to avoid direct interception, and that the remaining charge-exchange interception can also be reduced substantially by ion-optical means, particularly by using systems with high perveance and by employing an additional "diverter" electrode. The concept of "perveance-density matching" has been introduced in order to accommodate a nonuniformity of the ion current density available from a plasma-type source, and the effectiveness of this principle has been demonstrated.

I. Introduction

THE problem of extracting ions from a plasma and accelerating them with minimum interception on the accelerator electrode is an old one, having occurred, for example, in the design of ion sources for ion accelerators.[1–3] More recently, it has become important in the development of ion thrustors for the propulsion of space vehicles.[4] In an ion thrustor, it is particularly important to extract relatively high ion current densities with extremely low interception in order to minimize sputtering erosion of the accelerator electrode and make feasible lifetimes in excess of 10,000 hr.

The qualitative features of the process of ion¶ extraction from a plasma were described several years ago by Thoneman[5] and others,[6] who showed that the shape of the plasma boundary in the ion extraction region adapts itself to the applied extraction voltage and to the ion arrival rate from the plasma.

It is the purpose of Part I of this paper to establish quantitatively the conditions determining the position of the plasma boundary in an ion extraction system, to describe new concepts devised to overcome the specific problems encountered with ion extraction from plasma-type sources, and to report on the experimental verification of these concepts. The combination of these concepts with classical techniques[7, 8] of electron and ion dynamics has led to low-interception, high-perveance ion extraction and accelerating systems, which will be described in Part II, to be submitted for publication.

II. Theoretical Considerations

A. Sheath Formation and Plasma Boundary Conditions

It is known from the theory of probes[9] that, when an electrode is brought into contact with a plasma and held at a potential negative with respect to the plasma potential, an ion sheath is formed between the plasma and the surface of the electrode. To a first approximation, the transition from the plasma potential to the electrode potential takes place entirely within the ion sheath, whereas the plasma remains at a uniform potential. The potential gradient within the ion sheath causes an ion current to flow toward the electrode; in order to maintain continuity, this current must be drawn from the plasma through the boundary surface separating the quasi-neutral plasma region from the ion space-charge region.

Let us assume that the equilibrium position of the plasma boundary S is represented by those values $\mathbf{r}_S$ of the position vector $\mathbf{r}$ which satisfy a certain equation

$$F_S(\mathbf{r}) = 0 \tag{1}$$

The equilibrium position is then determined as follows: Because S is part of a plasma, it must, by the definitions of a plasma, be an equipotential surface,

$$V(\mathbf{r}_S) = \text{const} = V_{\text{plasma}} \tag{2}$$

and, by the same definitions, the inner surface (plasma side) of S must be field free:

$$\text{grad}\Big|_{\substack{\text{inner surface}\\ \text{of } S}} V(\mathbf{r}) = 0 \tag{3}$$

Because S is supposed to be in an equilibrium position, the forces acting on it must cancel at each point, and since, according to Eq. (3), S is not supported by (electrostatic) forces on its plasma side, the outer surface (sheath side) of S must also be force free, or

$$\text{grad}\Big|_{\substack{\text{outer surface}\\ \text{of } S}} V(\mathbf{r}) = 0 \tag{4}$$

Equations (3) and (4) may be combined in

$$\mathbf{E}(\mathbf{r}_S) = 0 \tag{5}$$

This equation, in combination with Eq. (2), states the necessary and sufficient conditions for the equilibrium of a plasma boundary; stated in words, these conditions are simply that S must be a field-free equipotential surface at the plasma potential.

The question then arises as to how (4) can be satisfied in the presence of an ion current through S. The answer is: 1) in order to produce a surface on which the potential has an extremum [that is, where grad $V(\mathbf{r})$ vanishes], this ion current must be space-charge limited in the sheath region;[10] and 2) in order to let this potential extremum coincide with S, the local space-charge limited ion current density $\mathbf{J}_{i,s\text{-}c}(\mathbf{r}_S)$

Presented in part as Preprint 64-8 at the AIAA Aerospace Sciences Meeting, New York, January 20–22, 1964; revision received May 26, 1964. This work was partially supported by the NASA Lewis Research Center.

* Member, Technical Staff, Plasma Physics Department; presently on leave to University of California at Los Angeles.

† Senior Staff Physicist, Plasma Physics Department. Member AIAA.

‡ Manager, Plasma Physics Department. Member AIAA.

§ Senior Associate Enginer, Ion Propulsion Department.

¶ Because this paper is concerned with positive ions only, the term "ion" is used with the exclusive meaning "positive ion."

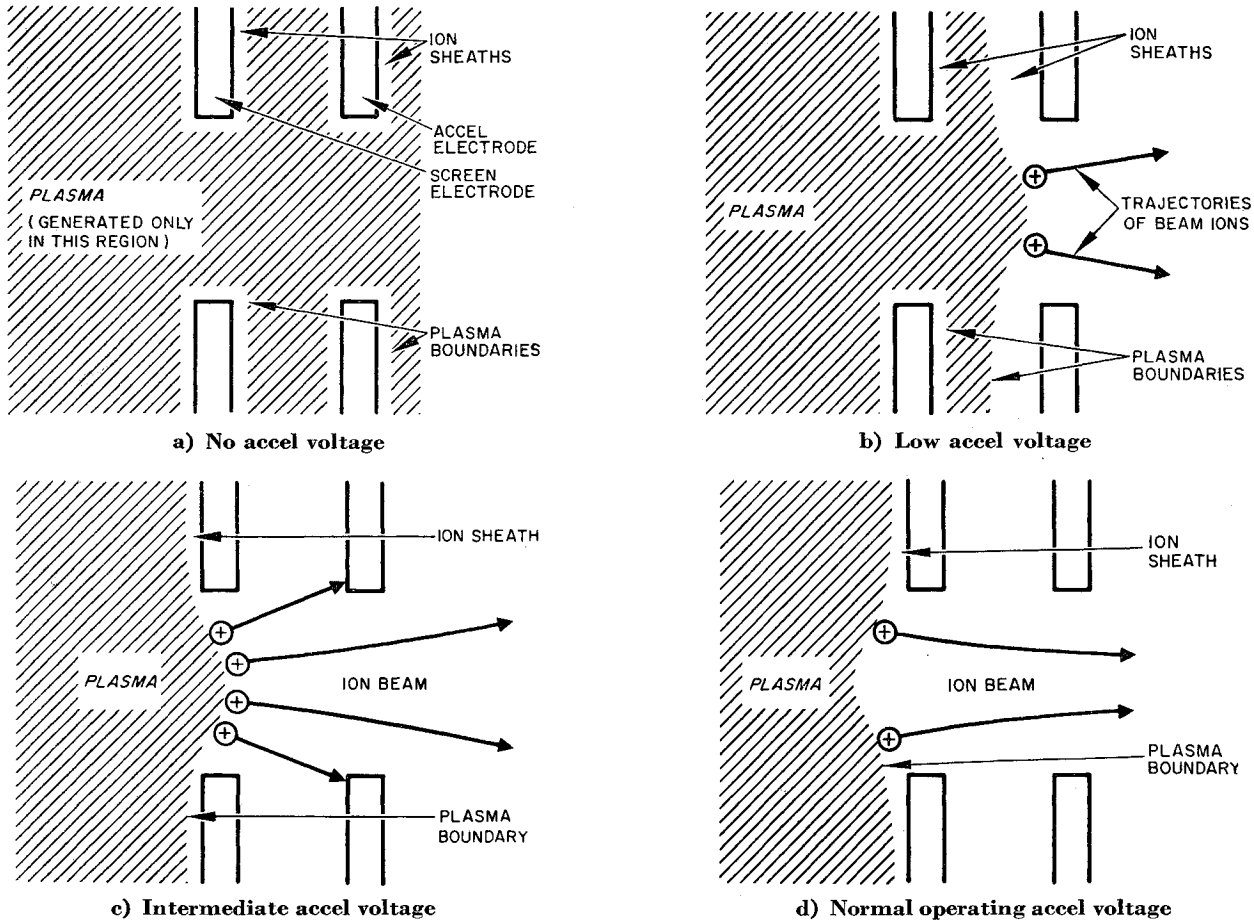

Fig. 1 Plasma boundary positions in an ion extraction system for various values of the accel voltage at constant plasma density.

must equal the maximum (saturation) ion current density $J_{i,\mathrm{sat}}(\mathbf{r}_S)$ locally available from the plasma:

$$\mathbf{J}_{i,s\text{-}c}(\mathbf{r}_S) = \mathbf{J}_{i,\mathrm{sat}}(\mathbf{r}_S) \tag{6}$$

The latter statement must hold because, if $J_{i,s\text{-}c}(\mathbf{r}_S)$ were greater than $J_{i,\mathrm{sat}}(\mathbf{r}_S)$, forementioned condition 1 would be violated, and if $J_{i,s\text{-}c}(\mathbf{r}_S)$ were less than $J_{i,\mathrm{sat}}(\mathbf{r}_S)$, some of the ions arriving at S would have to be reflected back into the plasma, thus requiring the existence of an electric field adjacent to S, in violation of (4).

Equations (2, 3, and 6) form an alternate set of necessary and sufficient conditions for an equilibrium position of a plasma boundary. In fact, they form a set of greater practical significance than Eqs. (2) and (5). This will immediately be appreciated when one realizes the analogy of Eqs. (2) and (3) to the electrostatic boundary conditions on a metal surface. It follows that the shape of a solid, metallic emitter that is operated simultaneously space-charge and saturation limited (CAS) [to satisfy Eq. (6)] also represents an equilibrium position for a plasma boundary under otherwise identical conditions.

A first application of this analogy is that, for a given potential difference ΔV between a plasma and an electrode and for given values of $J_{i,\mathrm{sat}}(\mathbf{r})$, the local sheath width [i.e., the distance $d(\mathbf{r}_S)$ between the plasma boundary and the electrode surface] can be written as follows [using the rationalized meter-kilogram-second-ampere (MKSA) system]:

$$d(\mathbf{r}_S) = \tfrac{2}{9}\epsilon_0^{1/2}(2q_i)^{1/4}m_i^{-1/4}(\Delta V)^{3/4} \times [J_{i,\mathrm{sat}}(\mathbf{r}_S)]^{-1/2}[1 + f(\text{geom at } \mathbf{r}_S)]^{1/2} \tag{7}$$

Here ϵ_0 is the permittivity of vacuum, q_i and m_i are charge and mass of the ions, respectively, and the function f(geometry at $\mathbf{r}_S$) vanishes if the plasma is homogeneous and the electrode is plane. Equation (7) results from expressions by Langmuir and Blodgett[11] for the space-charge limited current density between metal electrodes of various geometries and of local distance $d(\mathbf{r})$; these expressions can be summarized as

$$J_{i,s\text{-}c}(\mathbf{r}) = \tfrac{4}{9}\epsilon_0(2q_i)^{1/2}m_i^{-1/2}(\Delta V)^{3/2} \times [d(\mathbf{r})]^{-2}[1 + f(\text{geom at } \mathbf{r})] \tag{8}$$

Equation (8) was derived under the assumption of zero thermal velocities of the particles emitted by the metallic emitter, an assumption that also leads to Eq. (6), in this case not as a consequence of Eq. (4), but because partial reflection of an excessive saturation current by a potential barrier is possible only if the arriving particles possess a velocity distribution.

It should be noted that the concepts of a distinct plasma boundary and of a well-defined sheath width are applicable only if $d(\mathbf{r}_S)$, computed from Eq. (7), is large compared with the Debye length of the plasma:

$$\lambda_D(\mathbf{r}_S) = (\epsilon_0 kT_e/n_e e^2)^{1/2} \tag{9}$$

where k is Boltzmann's constant, e the electronic charge, and T_e and n_e denote electron temperature and number density, respectively.

Also, the different effects of thermal particle velocities in the cases of a plasma boundary and of a metallic emitter surface should be pointed out: A metal can balance by internal lattice forces the electrostatic forces acting on its surface; therefore, Eqs. (4) and (6) need not be satisfied, and nonvanishing thermal velocities result in a separation between the emitter surface and the potential extremum caused

by space-charge limited operation. In the plasma case, on the other hand, although the net force on S must always vanish [resulting in Eqs. (4) and (6)], the surface S will be randomly displaced by amounts of the order of the Debye length from its position for vanishing thermal velocities.

Consider now the case of two electrode plates, with apertures large compared with the Debye length, immersed in a plasma as shown in Fig. 1a. It is customary (for reasons that will soon become obvious) to call the electrode adjacent to the plasma generation region the screen electrode, and that on the other (downstream) side the accelerator (or accel) electrode. As long as both electrodes are at the same potential, slightly negative with respect to the plasma, the ion sheaths on both electrode surfaces are relatively thin and the plasma diffuses through both apertures.

Suppose now that an accel voltage (that is, a potential difference between the screen and accel electrodes) is being applied. As the accel electrode is made successively more negative, the sheath thickness at its surface increases. It then becomes comparable to the aperture diameter, and at a certain potential difference between the electrodes, the sheaths surrounding opposite edges of the accel aperture meet, leading to the situation of Fig. 1b. Here the plasma is no longer penetrating the accel aperture, and a divergent ion beam begins to emerge from it.

As the accel electrode is made still more negative, the plasma boundary recedes farther, the accel and screen electrode sheaths merge, and the situation shown in Fig. 1c is reached. The plasma region is now limited to the upstream side of the screen electrode, and the plasma boundary extending across the screen aperture is convex (as seen from outside of the plasma). The ion current flowing to the accel electrode is greatly reduced compared with the case of Fig. 1b, and now results entirely from interception of the (still divergent) ion beam passing through the accel aperture. This interception can be diminished very substantially by a further increase in accel voltage, causing the plasma boundary to change its shape within the screen aperture from convex to concave (see Fig. 1d). This situation is the one of interest for applications requiring long electrode life and is the subject of the following discussion.

B. Basic Ion-Optical Design Concepts

The obtainable current density and/or the life of systems for the extraction and acceleration of ions from plasma-type sources is limited by electrode erosion due to interception of energetic ions in optically critical locations, such as the edges of the accel apertures. The following mechanisms may contribute to this interception:

1) Direct interception due to an optically improper equilibrium shape of the plasma boundary. This effect is particularly pronounced if the extraction system is not matched to the nonuniformity of the saturation ion current density across the extraction area of the source.

2) Direct interception due to high random arrival velocities of the ions at the plasma boundary.

3) Charge-exchange collisions of the extracted and accelerated ions with neutral atoms escaping from the ion source, and subsequent interception of the secondary ions created by these collisions.

To minimize the effects of these mechanisms, we have evolved several concepts that are outlined below.

1. *Metallic-emitter analogy*

The first problem in the systematic design of an ion-optical system with minimum accel electrode interception is that of finding geometries for the screen and accel electrodes which, for a given set of operating parameters, will cause the plasma boundary to assume an optically favorable shape.

This task is considerably alleviated by the analogy (pointed out in the preceding section) that exists between the boundary conditions for plasmas and for solid, metallic emitters in CAS operation. In principle, this analogy is not limited to cases of uniform emitter current density; it requires only that Eq. (6) be satisfied at each point on the emitter surface. However, previous designs of ion-optical systems for metallic emitters have been subject to the condition of uniform emitter saturation current density, and therefore this restriction does exist regarding the practical value of the analogy. In cases of nonuniform saturation ion current density, however, the condition of uniform emitter current density can be satisfied by an appropriate subdivision of the total available extraction area (see Sec. II-B-5); therefore, the design of optimum ion extraction systems for plasma-type ion sources can make use of systems already developed for metallic ion emitters. In fact, the potential distribution and the ion trajectories of an ion-optical system with a solid, metallic emitter giving uniform current density in CAS operation are, in first approximation, identical to those of the same system with the same accel voltage when a plasma, capable of supplying the same ions at the same saturation current density, is substituted for the metallic emitter.

2. *Electrolytic-tank analog representation*

The fields and trajectories of ion extraction systems can be studied using an analog representation of electrostatic fields in electrolytic tanks, based on the fact that the electric potential obeys Poisson's equation in electrostatic space-charge fields as well as in stationary current fields with distributed current sources, only with different meaning of the source term and the constants. Such tanks have been used very successfully for the design of ion-optical systems with metallic emitters, and are, therefore, on the basis of the metallic-emitter analogy, also an important tool for the design of extraction systems for plasma-type sources.

Moreover, it is also possible to use an electrolytic tank without a solid emitter electrode, and to find the equilibrium position of the plasma boundary by identifying it with the surface within the current field which satisfies Eqs. (2, 3, and 6). This technique permits the simulation of the one important characteristic of a plasma boundary by which it differs from a solid emitter: its change of shape and position in response to changes in the operating parameters.

3. *Operating-perveance dependence of interception*

As shown in Sec. II-A, the surface of a metallic emitter designed for CAS operation at uniform current density also represents the stable position of a plasma boundary for the design set of operating parameters. However, this is but one of many positions which the boundary can assume when subject to changes of the accelerating voltage or of the saturation ion current density available from the plasma. If either the accel voltage is increased while the plasma density is held constant or the plasma density is decreased while the accel voltage is held constant, the plasma boundary will recede farther from the accel electrode until Eq. (6) is again satisfied. This results in changes of the perveance** of the ion-optical system formed by the plasma boundary and the electrodes and, of course, in changes of the ion trajectories. Consequently, by determining for an ion-optical system the dependence of accel interception current and total beam current on accel voltage, and by representing the relative accel interception†† as a function of the operating perveance,

** Perveance is defined as the ratio (space-charge limited current)/(accel voltage)$^{3/2}$. It follows from Eq. (8) that the perveance is a scale-invariant property of an optical system for charged particles, depending only on the geometry of the system and on the charge and mass of the particles. The MKSA unit of perveance is 1 perv = 1 AV$^{-3/2}$.

†† Relative accel interception is the ratio (accel interception current)/(total beam current).

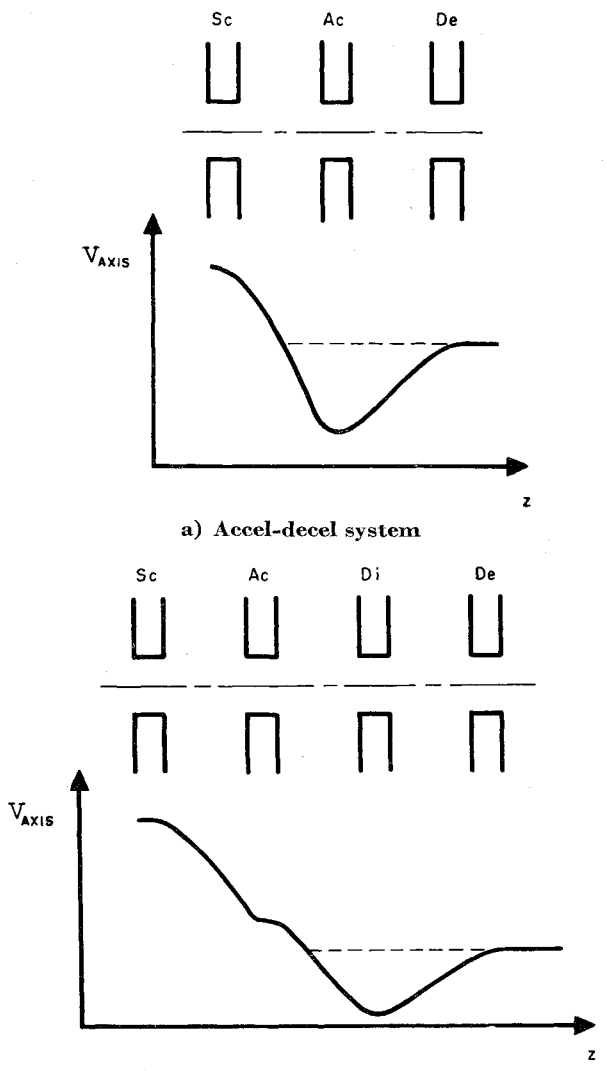

Fig. 2 Schematic potential distributions on the axis of ion extraction systems with and without a diverter electrode. (*Sc* = screen, *Ac* = accel, *Di* = diverter, *De* = decel electrode.)

one can determine the maximum deviation from the design current density at a given accel voltage which is permissible in the use of the system.

4. *Effect of sheath width at screen electrode*

Within the center part of a screen aperture, the shape of the plasma boundary for a given saturation ion current density depends only on the potential difference between plasma and accel electrode; the plasma boundary shape near the screen aperture edge, however, is also affected by the width of the sheath adjacent to the screen electrode. The dependence, in turn, of this sheath width on the saturation ion current density and on the potential difference between plasma and screen electrode is given by Eq. (7). The effect of this sheath width on perveance and relative interception (as functions of accel voltage) may be quite important in practical cases.

It is easy to draw the conclusion that the screen sheath width should be kept small compared with the screen aperture width from the following qualitative argument: An ion beam which is to pass through the accel aperture with low interception must be extracted from a generally concave plasma boundary. However, if the plasma boundary is concave in the center of the screen aperture, it must be convex near the aperture edges (see Fig. 1d). To keep the interception low, the convex part of the plasma boundary should be small compared with the concave part, a requirement that leads directly to the foregoing conclusion.

5. *Perveance-density matching*

The specified accel voltage and the local saturation current density of a plasma-type ion source impose the local value of the operating perveance density‡‡ on the extraction system. To obtain low accel interception with a source exhibiting a substantial nonuniformity of its saturation current density across the extraction area, it is necessary to match locally the design perveance density of the extraction system to the imposed operating perveance density.

This requirement can be reconciled with the restriction of existing ion-optical designs to uniform emitter saturation current density, provided the extraction system is subdivided§§ into an array of ion-optical elements,¶¶ and further, provided that this subdivision is done in one of the following two ways: If ion-optical elements with two-dimensionally convergent ion flow are used (for example elements consisting of circular apertures), the individual screen apertures must be small enough to render negligible the variation of saturation current density within each aperture. If, on the other hand, ion-optical elements with one-dimensionally convergent flow (for instance, elements consisting of oblong apertures) are employed, the condition of nearly constant saturation current density must be satisfied only with respect to the direction of flow convergence, whereas perpendicular to it the dimensions of the element may be a function of position, as required for perveance-density matching.

In either case, there are in principle two possibilities for achieving the match: the local design perveance* may or may not be kept constant as the geometry of the elements is varied as a function of position. Systems that use a uniform local design perveance have the obvious advantage of requiring only a single ion-optical design, which is subsequently scaled as a function of the local saturation current density: Let b denote any characteristic linear dimension of an element, and let $\mathbf{r}_0$ be the position vector to that point on the extraction surface for which the design was made; then, as a consequence of Eq. (8), the scaling law is

$$\frac{b(\mathbf{r}_S)}{b(\mathbf{r}_0)} = \left[\frac{J_{i,\mathrm{sat}}(\mathbf{r}_0)}{J_{i,\mathrm{sat}}(\mathbf{r}_S)}\right]^{1/2} \tag{10}$$

It should be noted, however, that in practical cases, perveance-density matching with uniform local design perveance may not be possible if elements employing two-dimensionally convergent flow are used. Circular apertures, for example, may become so large in the low-current-density regions of

‡‡ We define "perveance density" as the ratio (space-charge limited current density, referred to the projection of the emitter area on a plane normal to the beam)/(accel voltage)$^{3/2}$. The perveance density of a system is inversely proportional to the square of its linear scale; see Eq. (8).

§§ Subdivision of the extraction area is necessary in space propulsion applications, even for non-perveance-density-matched systems, because of the typical mission-imposed parameters.

¶¶ The term "ion-optical element" is used herein for an ion-optical system with a single aperture in each electrode.

* We define "local perveance" as follows: if the ion-optical array consists of elements employing two-dimensionally convergent flow, the local perveance is the perveance of a specific one of these elements; if the array consists of elements employing one-dimensionally convergent flow, the local perveance is the perveance of a square section of the actual element, the sides of this square being equal to the width of the screen aperture in the direction of flow convergence. It follows from the scale-invariance of perveance [or directly from Eq. (8)] that the so-defined local perveance is also scale-invariant.

the extraction area that the saturation current density already varies appreciably within one screen aperture.

6. *Effect of initial ion velocities*

The random thermal velocities with which ions leave a metallic contact ionizer kept, for instance, at $\approx 1000°K$ do not pose an ion-optical design problem in propulsion applications because they are sufficiently small compared with typical exhaust velocities. It is not obvious whether this statement should also apply to ions created in discharge-type sources, because here the ions may arrive at the plasma boundary with much higher and possibly random velocities, with an upper limit corresponding approximately to the discharge voltage. For the discharge voltages normally encountered, it follows from the relation $1 \text{ ev} \hat{\approx} 10^4 °K$ that these velocities may be more than an order of magnitude higher than in the thermal-emitter case. Therefore, a careful ion-optical design procedure for discharge-type sources should include a check (in the electrolytic tank) that even ions arriving at the plasma boundary with a velocity of the most unfavorable magnitude and direction will not be intercepted by the accel electrode.

7. *Diversion of charge-exchange ions*

The interception of ions created by charge-exchange collisions (abbreviated to "charge-exchange ions") is of particular importance in space propulsion applications where neutralization of the ion beam by electrons is required. To prevent the backstreaming of neutralizing electrons into the ion source, the potential distribution within the optical system of an ion thruster must contain an electron barrier, that is, a potential minimum, usually created by mounting a decelerator (or decel) electrode downstream from the accel electrode and keeping its potential between the screen and accel potentials (Fig. 2a).

Such a potential distribution constitutes a trap for charge-exchange ions that are generated in the region of lower-than-decel potential, indicated by the dashed line in Fig. 2a. Being unable to escape from the potential well, but able to move in three dimensions (rather than the one dimension of Fig. 2), most of these ions are intercepted by the accel electrode, thus limiting by sputtering erosion the useful life of this electrode.

Obviously the trap region, and therefore the accel-decel voltage ratio, should be kept as small as possible to minimize this effect. A considerable further reduction in accel charge-exchange interception can be expected, however, from a potential distribution as shown in Fig. 2b.† Here, an additional ("diverter") electrode is inserted between the accel and decel electrodes, and this diverter electrode is kept at the lowest potential of the system. The accel-decel voltage ratio may now be less than unity (as shown in Fig. 2b), in which case none of the trapped charge-exchange ions will be able to reach the accel electrode. Even at accel-decel ratios greater than one, however, the accel charge-exchange interception should be reduced substantially.

The name diverter was chosen because this electrode diverts onto itself most of those charge-exchange ions that would otherwise impinge on the accel electrode. This is done, of course, at the expense of subjecting the diverter electrode to sputtering erosion. However, since the shape of this electrode has only a negligible influence on the field geometry within the beam-forming region (between screen and accel electrode), it may be eroded to a much higher degree than the accel electrode before a comparable increase in total beam interception will result.

It should be noted that not all features of charge-exchange interception can be illustrated by the one-dimensional Fig. 2. For instance, not only charge-exchange ions that were generated within the potential well can reach the accel electrode. It can be expected, though, that by designing an accel-diverter-decel system with the aid of an electrolytic tank, a substantial fraction of all charge-exchange ions that would normally erode the accel electrode in optically critical locations can be diverted so that they either impinge on the diverter electrode or, at least, hit only noncritical regions of the accel electrode.

A side effect of choosing a potential distribution according to Fig. 2b, rather than Fig. 2a, is the requirement for a higher design perveance density, if the same current density and exhaust velocity (as determined by the decel voltage) are to be maintained. High perveance density, on the other hand, requires high local perveance, as a consequence of breakdown limitations. Thus, the requirement for reducing charge-exchange interception necessitates the evolution of ion-optical systems with high local perveance.

III. Procedures of Investigation

A. Electrolytic-Tank Studies

An electrolytic tank with a movable field-sensing probe, coupled to an analog computer, had been developed previously at the Hughes Research Laboratories[3] and was available for this investigation. In this tank, the probe is electromechanically driven by the output of the computer to describe the trajectory of the charged particle considered. Space charge is simulated by injection of appropriate currents through auxiliary probes into the electrolytic tank.

Tanks with different cross sections are used, depending on the geometry of the problem: one-dimensionally convergent beams are simulated in a tank with uniform depth, whereas a wedge-shaped tank is used to simulate one segment of a two-dimensionally convergent flow field.

B. Ion Beam Measurements

For actual ion beam extraction experiments, a demountable electron-bombardment ion source (hot-cathode Penning discharge) was constructed.‡ In this source, a plasma is maintained within a cylindrical chamber by means of electron-impact ionization of the enclosed gas. The ionizing electrons are emitted from a centrally located thermionic cathode (in this case an axial filament) and are collected at a cylindrical anode (of 6.5-cm diam and 11.5-cm length in our apparatus). The cylindrical section is terminated by two end plates that are kept at cathode potential in order to trap the electrons in the axial direction. To decrease the mobility of the electrons in the radial direction, a magnetic field is maintained parallel to the axis. The magnitude of this axial magnetic field is such that the maximum cyclotron radius of the electrons is a fraction of the anode radius. One of the end plates also serves as the distributor for the expellant (argon and xenon in our experiments), whereas the other also acts as the screen electrode of the extraction system. The pressure inside the discharge chamber can be monitored by an ionization gauge connected to a probe line that penetrates the distributor end plate.

Figure 3 is a photograph of this source with an ion extraction system mounted on its downstream end plate, and Fig. 4 shows a schematic cross section of source and extraction system, as well as a diagram of the circuit used in the beam extraction experiments.

The insulators supporting the accel electrode of the ion-optical system are mounted on a guard ring that is kept at accel potential in order to prevent accel insulator leakage current from being measured as part of the accel electrode

† This idea was first conceived at Hughes Research Laboratories in 1961 by S. L. Eilenberg.

‡ This electron-bombardment source is similar to that first described by Kaufman.[4]

current. The function of the suppressor and shield electrodes is described in the following sections; they are auxiliary electrodes introduced to permit unequivocal measurements of the various interception currents. It should be understood that only four electrodes would be included in a practical ion extraction system: the screen, accel, diverter, and decel electrodes.

IV. Demonstration of Validity of Theoretical Concepts

A. Plasma Boundary Position and Effect on Accel Interception

1. Electrolytic-tank studies

Electrolytic-tank studies have been performed with the Hughes Research Laboratories (HRL) 24-G optical system, which had previously been designed as an electron gun for operation at uniform emitter current density. This system was selected because its potential and space-charge distribution and the particle trajectories were already known from prior investigations with the electrolytic tank for the case of a metallic emitter. A large-scale representation of the ion emitter was placed at its design position in the electrolytic tank. The space-charge distribution for CAS operation was simulated by means of the current injection probes between the emitter and accelerator electrode. The potential distributions, both with and without emitter electrode, were then measured in the tank for this system.§ As expected, it was found that the potential distribution was not perturbed by removal of the metallic emitter and that a field-free equipotential surface remained at the location previously occupied by the emitter electrode. This verified the equivalence of a solid, metallic emitter in CAS operation and of a plasma boundary for operation at the design perveance of this system. A plot of the equipotential surfaces measured both with and without the emitter electrode is shown in Fig. 5.

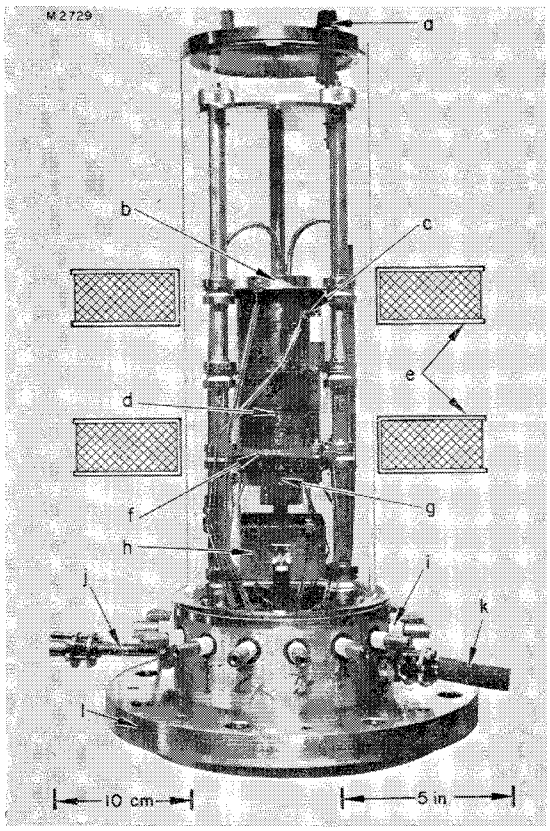

Fig. 3 Electron-bombardment source with ion-optical system and beam collector in vacuum bell jar; the magnet coils are shown in schematic cross section. (*a* = actuating knob for movable system, *b* = distributor end plate, *c* = filament feed-through, *d* = anode, *e* = Helmholtz coils, *f* = screen end plate, *g* = guard ring of extraction system, *h* = collector, *i* = electrical feed-throughs, *j* = discharge-chamber pressure probe line, *k* = expellant feed line, *l* = pump system flange.)

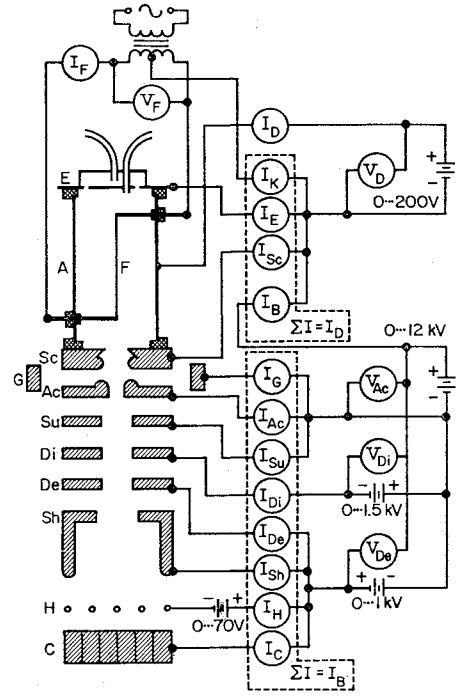

Fig. 4 Circuit diagram and schematic cross section of electron-bombardment source (same scale as Fig. 3) and six-electrode ion-optical system (not to scale). (*A* = anode, *B* = beam, *C* = collector, *D* = discharge, *E* = distributor end plate, *F* = filament, *G* = guard ring, *H* = suppressor grid, *I* = current, *K* = cathode, *V* = voltage; electrodes: *Sc* = screen, *Ac* = accel, *Su* = suppressor, *Di* = diverter, *De* = decel, *Sh* = shield.)

Having established that the plasma boundary shape and position can be determined with the electrolytic tank, we investigated the effect of perturbations on the position and shape of this boundary. Starting with the design perveance (the conditions in which the position of the simulated plasma boundary corresponds to the position of the solid emitter) and maintaining a fixed accel voltage, we increased the space-charge simulation currents in the electrolytic tank to simulate an increased saturation ion current density supplied by the plasma and a corresponding increase in ion beam current and in operating perveance. Consistent with this increased operating perveance, the surface of zero electric field (plasma boundary) was found to shift downstream. In order to conform to conditions prevailing within a plasma (zero average space charge), all space-charge simulation currents emanating from sources upstream from the plasma boundary were reduced to zero in the iterative procedure leading to the final plasma boundary position. For small increases in operating perveance, the edge of the ion sheath adjacent to the screen electrode shifts downstream along

§ The electrodes in the electrolytic tank consisted of sheet metal strips following the contours of the electrodes to be simulated. In the measurement "without emitter electrode," only the concave part of the emitter electrode contour was removed from the tank, in order to simulate the gap between plasma boundary and screen electrode caused by the ion sheath at this electrode (see Fig. 5).

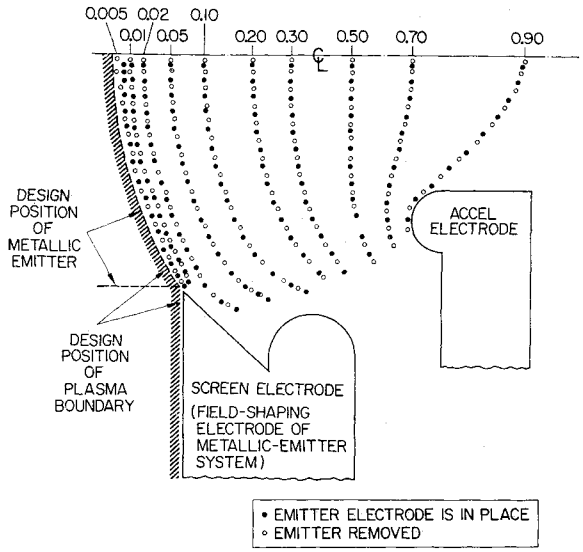

Fig. 5 Equipotential surfaces of HRL 24-G system with and without emitter electrode. (The electrode shapes are schematic.)

this electrode, and the plasma boundary becomes less concave. There is no immediate increase in direct accel interception, however, since all particles miss the accel electrode by a considerable margin under design conditions. Interception does begin to increase sharply for larger departures from the design perveance. We see in Fig. 6a that at an operating perveance of 2.5 times the design value the equipotentials have shifted considerably downstream from their position at design perveance, and the radius of curvature of the plasma boundary has increased to 2.25 times its value at design perveance. The space-charge-free trajectories are presented in Fig. 6b, and the space-charge-limited trajectories in Fig. 6c. These final space-charge-limited trajectories result in a relative accel interception of 43% for operation at 2.5 times design perveance.

2. *Ion beam measurements*

Screen and accel electrodes of the HRL 24-G system were installed on the electron-bombardment source described in Sec. III-B. The screen aperture of this system has a diameter of only 15% of the discharge chamber diameter, thus insuring operation sufficiently close to the design condition of uniform emitter current density. The source was operated with argon gas in a magnetic field of about 50 gauss and with a discharge voltage ranging from 50 to 100 v.

In these measurements, the relative accel interception could be minimized for given discharge parameters by optimizing the extraction voltage, i.e., by operating at an optimum extraction perveance. The interception current measured under these conditions varied linearly with the value of both the beam current and the argon pressure as measured in the discharge chamber; the pressures in the acceleration gap and in the region between accel electrode and collector are roughly proportional to the discharge chamber pressure. Such dependence indicated that the major part of the interception resulted from charge-exchange scattering that occurred both in the accel gap and between the accel electrode and the collector. The interception was as high as 4% at a chamber of 5×10^{-4} torr. This large value resulted because many of the charge-exchange ions created in the region between the accel electrode and the collector were able to return to the large inactive surface of the accel electrode. A shield electrode, masking the major part of the downstream surface of the accel electrode, was subsequently installed to prevent most of this return. Its installation reduced the minimum relative accel interception by more than an order of magnitude and thus made it possible to observe the contributions of ion-optical effects to interception.

To measure the effect of operating perveance on relative accel interception, the perveance was varied while the beam current was kept at a constant value of 1.3 ma. This was accomplished at various pressures by adjusting the accel voltage and the discharge current to achieve the desired operating perveance. The relative accel interception was then measured over a broad perveance range and plotted in Fig. 7. It is seen from these data that interception remains

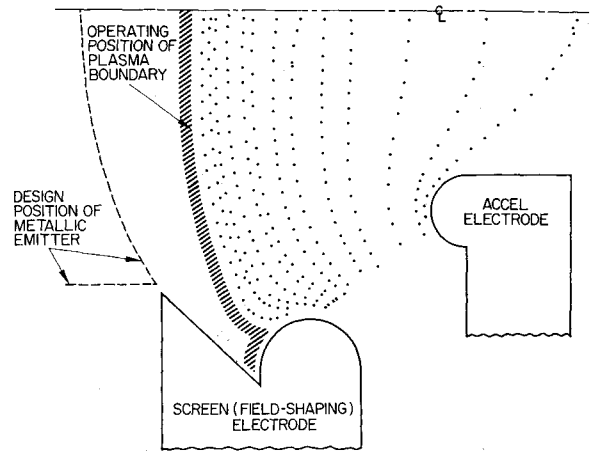

Fig. 6a Equipotential surfaces of HRL 24-G system operated at 2.5 times its design perveance.

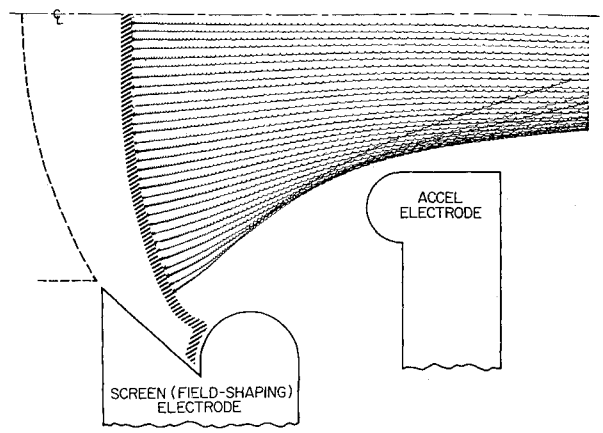

Fig. 6b Trajectories of HRL 24-G system operated without space-charge simulation at 2.5 times the design perveance.

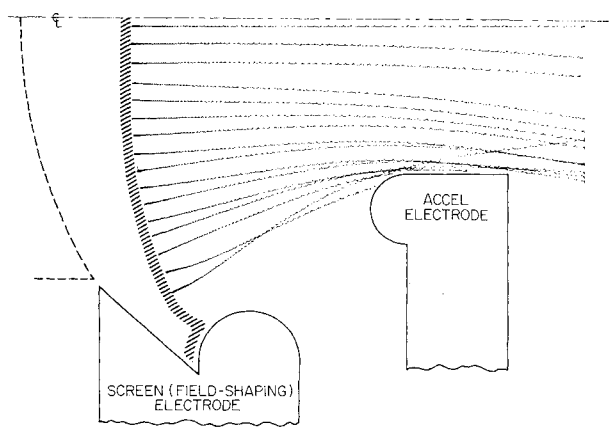

Fig. 6c Trajectories of HRL 24-G system operated with space-charge simulation at 2.5 times the design perveance. Such operation results in interception of 43% of the beam by the accel electrode.

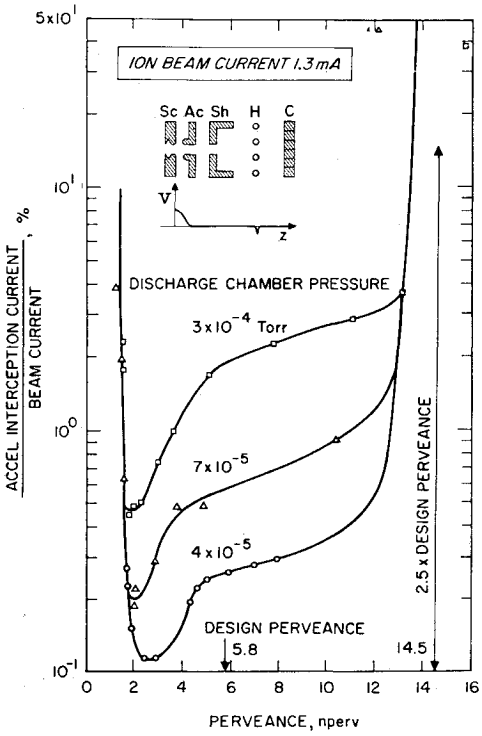

Fig. 7 Relative accel interception vs operating perveance of the HRL 24-G system. Parameter: discharge chamber pressure. The insert shows schematically the electrodes and potential distribution used.

at low values over a variation of ±50% from the design perveance. Beyond this range, interception rises steeply. At the high perveance limit, it is presumed that the plasma boundary bulges forward from its concave shape to a position where beam convergence is too slight and ions collide with the accel electrode. At the low perveance limit, the concavity of the sheath is too pronounced and the ion trajectories are so highly convergent that they cross the central axis and collide with the accel electrode on the side of the optical system opposite to that from which they came. For the perveance range within ±50% of the design perveance, direct interception is completely overshadowed by charge-exchange interception, as evidenced by the fact that the interception in this region is proportional to gas pressure. The total

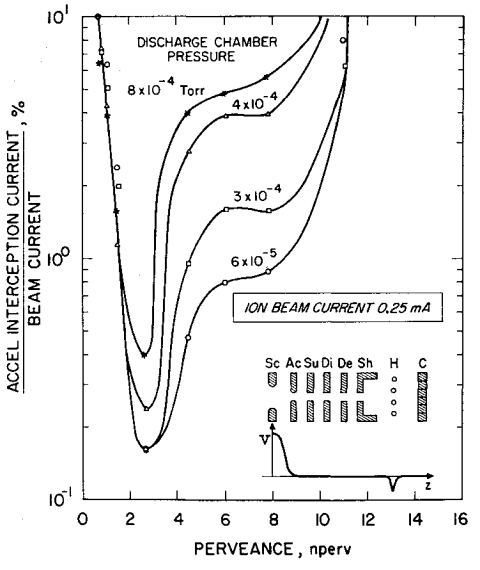

Fig. 8 Relative accel interception vs operating perveance of the flat-plate ion-optical system. Parameter: discharge chamber pressure.

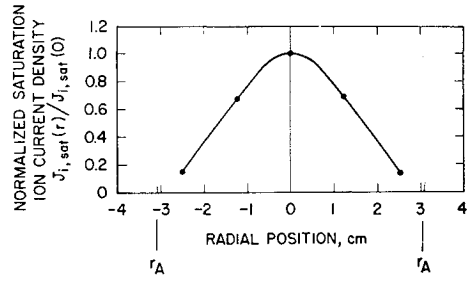

Fig. 9 Radial distribution of saturation ion current density. Discharge parameters: voltage 60 v, current 0.25 A, pressure 7 × 10⁻⁵ torr, expellant argon.

accel interception (direct, if any, plus charge-exchange) reaches its minimum at an operating perveance lower than the design perveance. This is to be expected because the stronger focusing field geometry prevalent at lower perveance helps to direct the charge-exchange ions through the accel aperture without interception.

It is interesting to compare the relative accel interception computed from trajectory tracings in the electrolytic tank with that actually measured in a range where ion-optical effects predominate over charge exchange. As reported in Sec. IV-A-1, the interception computed for operation at 2.5 times the design perveance was 43%. The interception actually measured for this condition is consistent with this value, as can be seen from Fig. 7.

To establish the effect of the sheath width at the screen electrode on interception, data were taken at constant beam currents of 0.25 ma and 3.4 ma. As before, the accel interception varied with operating perveance and chamber pressure. In addition, however, the interception minima showed a characteristic shift to higher perveance with operation at higher current density. This shift was predicted in Sec. II-B-4. At sufficiently high current densities, the screen sheath width becomes vanishingly small, and the operating perveance for minimum interception should approach the design perveance asymptotically. Such behavior has also been observed experimentally; data showing this effect are reported in Part II of this paper, to be submitted for publication.

To evaluate the effect of electrode geometry on interception, a simple flat-plate ion extraction geometry was compared with the HRL 24-G ion-optical system. This system was designed to retain as many of the relevant dimensions of the HRL 24-G system as was compatible with the use of flat plates. The observed characteristics were in many ways similar to the data for the HRL 24-G system, but with one important difference. As shown in Fig. 8, the minimum accel interception current is 1.6×10^{-3} of the beam current. This value remains constant as a function of pressure until the pressure rises above 3×10^{-4} torr. This indicates that the minimum of interception is limited to this value by direct interception, in contrast to the situation with the HRL 24-G system where direct interception in the vicinity of the design perveance was so low that it remained immeasurably small down to the lowest gas pressure used.¶

¶ It may be noted that charge-exchange interception appears lower with the flat-plate system (data of Fig. 8) than with the HRL 24-G system (data of Fig. 7). This is apparent from the fact that at a pressure of 3×10^{-4} torr charge-exchange interception in the flat-plate system is lower than the total interception of 0.16%, whereas for the HRL 24-G system charge-exchange interception completely predominates and is 0.5% at the same pressure. The reason is that the six-electrode system used for the flat-plate measurements provides better shielding from the return of charge-exchange ions to the accel electrode than the three-electrode system used for the HRL 24-G measurements. This has been substantiated by measurements performed with the HRL 24-G system in the six-electrode configuration, showing reduced charge-exchange interception (see Fig. 12).

The conclusion of this test is that direct interception is definitely affected by the electrode geometry. Although with the HRL 24-G system direct interception could be made so small that it became negligible, with the flat-plate system this was not possible. Because in an optimum design it is necessary to minimize both charge-exchange interception and direct interception, exact design of the electrode shapes based on electrolytic-tank trajectory tracings is most important.

B. Demonstration of Perveance-Density Matching

1. Measurement of radial distribution of saturation current density

The normal screen electrode of an electron-bombardment source was replaced by one perforated with three holes of 0.15-cm diam, located at $\frac{1}{5}$, $\frac{2}{5}$, and $\frac{4}{5}$ of the discharge-chamber anode radius. Crossed-wire 200-wire/cm nickel meshes were placed over the apertures to limit the penetration of the extraction fields and to define a uniform position for all three plasma boundaries. Three solid extraction electrodes were placed downstream from the screen electrode directly opposite to these holes. The extracted ion currents rose rapidly to a saturation value at a voltage as low as 50 v. The radial variation obtained from these measurements amounts to almost an order-of-magnitude dropoff in saturation ion current density from the center to the edge of the discharge and is plotted in Fig. 9. This radial distribution varied somewhat with discharge chamber operating conditions, becoming more uniform at higher discharge voltage and lower discharge currents, but under any conditions at least a 3:1 dropoff was observed from the center of the discharge to the position at $\frac{4}{5}$ of the anode radius.

The conclusion is that the operating perveance density of the extraction system must vary as a function of radial position over a range exceeding the low-interception limits of a system with uniform design perveance density; therefore, perveance-density matching is necessary for optimum ion extraction.

2. Matching with movable system

The ion-optical system used in our experiments was designed so that it could be moved radially across the discharge chamber by actuation from outside of the vacuum system. This capability has allowed us to demonstrate that the radial variation in saturation ion current density can be accommodated by operating the extraction system at its optimum perveance for all desired radial positions. An ion beam was extracted at constant perveance from five points across the discharge (at the center and at $\frac{1}{5}$, $\frac{2}{5}$, $\frac{3}{5}$, and $\frac{4}{5}$ of the distance from the center to the anode). The beam current was found to decrease with radius as before, but the relative interception remained at a uniformly low value so long as the perveance was kept approximately constant by adjusting the accel voltage to accommodate the variation in beam current. Measurements of accel interception vs operating perveance at each radial position yielded the same relationship as at the center of the discharge.

These results show that it is actually possible to achieve perveance-density matching for minimum interception at all radii. In a practical situation, of course, instead of adjusting the accel voltage as a function of radius, the dimensions of the system must vary as a function of radius as described in Sec. II-B-5.

C. Effect of Initial Ion Velocities

The effect of initial ion velocities has been studied with the electrolytic-tank trajectory tracer to determine its importance to accel interception in the HRL 24-G system. Figure 10 shows the trajectories of ions started from the beam edge with initial velocities corresponding to 3% of the accel voltage, at angles of 0°, 15°, 30°, and 45° to the beam axis. It was found that particles injected at 15° to the axis made the nearest approach to the accelerator electrode. It was then determined that a particle injected in this direction required an initial velocity corresponding to 4% of the accel voltage to reach the accelerator electrode. Since this is an upper limit for the discharge voltage which will not be reached in normal ion-thrustor operation, one would not expect initial ion velocities to affect accel interception in the investigated system.

D. Diversion of Charge-Exchange Ions

1. Electrolytic-tank studies

Most of the neutral atoms participating in charge-exchange collisions have arrival velocities that are very small compared with those of the beam ions, and therefore most of the charge-exchange ions are created with similarly low initial velocities. This consideration is the basis for the investigation of charge-exchange interception with the aid of the electrolytic tank: to simulate the trajectory of a charge-exchange ion created at an arbitrary point within the beam boundary, the field-sensing probe describing the particle trajectory is simply started with zero initial velocity from that point.

To demonstrate the utility of this technique, a study of charge-exchange trajectories within the HRL 24-G system (without any additional electrodes for deceleration and diversion) has been made. The result, emphasizing a remark made in Sec. II-B-7, is that, even for a potential distribution containing no trap region for charge-exchange ions, two distinct regions exist in the accelerated ion beam: charge-exchange ions generated in the region close to the plasma boundary are adequately refocused by the ion extraction system and pass through the accel aperture without being intercepted; charge-exchange ions generated in the other region are intercepted by the accelerator electrode. These two regions are shown in Fig. 11, together with a few critical charge-exchange ion trajectories.

In the trajectory study illustrated by Fig. 11, the downstream end of the region contributing to accel interception was left undefined. In an actual system, the position and shape of this downstream termination are determined by the geometry and potentials of the downstream electrodes. Because the complex electrode shapes of the HRL 24-G system make it rather impractical as an element of an ion extraction array, the detailed electrolytic-tank study of decel and diverter electrode effects was limited to the more practical geometry of the optimized element described in Part II. Preliminary experiments with decel and diverter electrodes

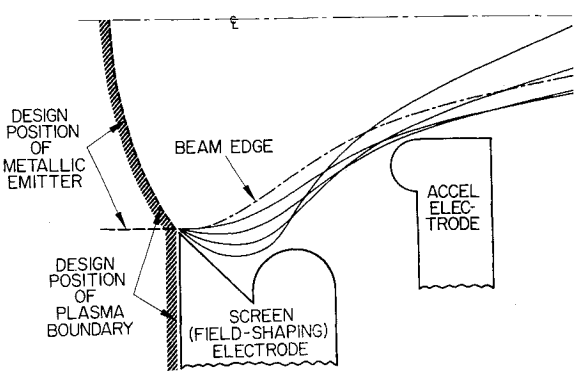

Fig. 10 Study of the effect of initial ion velocities on beam trajectories of HRL 24-G system. Trajectories with initial velocities corresponding to 3% of accel voltage are plotted for 0°, 15°, 30°, and 45° starting angles relative to the beam axis. The minimum velocity that causes accel interception is 4% of the accel voltage at a 15° starting angle.

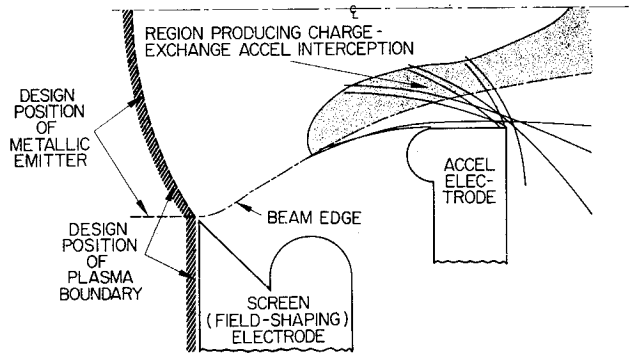

Fig. 11 Trajectories showing the accel interception induced by charge-exchange scattering in the HRL 24-G system. Pairs of critical trajectories are shown which determine the boundary of the region producing charge-exchange accel interception.

added to the HRL 24-G system did indicate, however, that the size of the generation region for accel-interception ions can be reduced substantially by the use of a diverter electrode.

2. *Ion beam measurements*

To study decel and diverter effects, a decel, a diverter, and a suppressor electrode, all consisting of flat plates with circular apertures, were installed between the shield and the accel electrode of the HRL 24-G system. The purpose of the suppressor electrode, mounted between diverter and accel electrodes, was to prevent secondary electrons produced on the diverter electrode from being collected by the accel electrode and thus obscuring accel ion interception readings.

To establish the effect of decel potentials, all electrodes downstream from the accel electrode were joined electrically to a common potential, which was varied from 0 to 900 v positive relative to accel potential. Figure 12 shows the increase of accel interception with increasing accel-decel potential difference over the full operating perveance range of this ion extraction system. These data were taken at a constant ion beam current of 0.25 ma and represent operation at accel voltages between 1 and 9 kv. Note that the

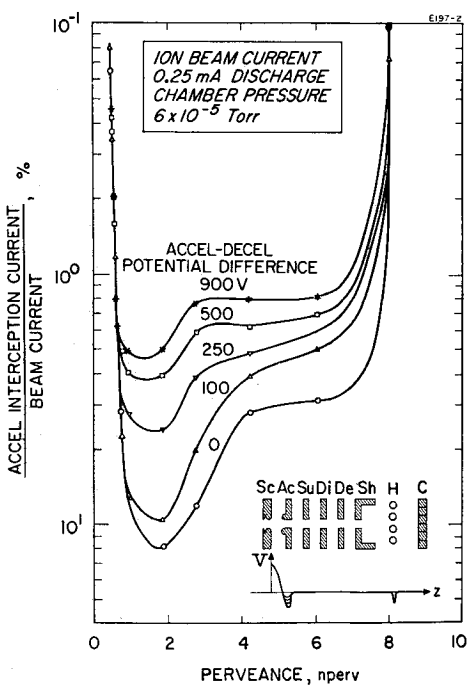

Fig. 12 Relative accel interception vs operating perveance of the HRL 24-G system. Parameter: accel-decel potential difference.

minimum accel interception for zero accel-decel potential difference was reduced from that shown in Fig. 7 by the increased shielding provided by the additional downstream electrodes.

To observe the effect of the diverter electrode, the electrodes were biased as shown schematically in Fig. 2b. With the decel and shield electrodes held 500 v positive with respect to accel potential, the diverter electrode was set at various potentials negative with respect to the accel electrode. With the diverter at accel potential, the effect of decel potentials was essentially unaltered. As the diverter was made more negative, accel interception generally decreased; the decrease was not linear, however, nor even monotonic with changing diverter potential. As in the electrolytic-tank studies, the effort to obtain optimum diverter performance was applied to the optimized element described in Part II rather than to the HRL 24-G system.

V. Conclusions

The following conclusions can be drawn from the results presented herein:

1) A technique has been developed which permits electrolytic-tank trajectory-tracer simulation of ion-optical systems for the extraction and acceleration of ions from a plasma. The position of the plasma boundary can be accurately determined by this technique, and the corresponding ion trajectories can be obtained. It is now possible, therefore, to use an electrolytic tank for the systematic design of optimized ion-optical systems for extraction and acceleration of ions from a plasma.

2) For operation in the vicinity of the design perveance of a well-designed ion-optical system, it has been conclusively established that accel interception is predominantly due to charge-exchange ions. Departure from operation at the design perveance by an amount depending on the system geometry increases direct interception to a point where it becomes predominant.

3) It should be possible to achieve low accel interception by means of the following techniques: a) design of an extraction system of high ion-optical quality (to avoid direct interception) and with high local perveance (to permit operation at low accel-decel ratios); b) diversion of charge-exchange ions to an ion-optically noncritical diverter electrode; and c) perveance-density matching of the ion-optical system to the saturation current-density distribution of the ion source.

References

[1] Finkelstein, A. T., "A high efficiency ion source," Rev. Sci. Instr. **11**, 94–97 (1940).

[2] Heil, H., "Ueber eine neue Ionenquelle," Z. Physik **120**, 212–226 (1943).

[3] Thoneman, P. C., Moffat, J., Roaf, D., and Sanders, J. H., "The performance of a new radio-frequency ion source," Proc. Phys. Soc. (London) **61**, 483–485 (1948).

[4] Kaufman, H. R., "An ion rocket with an electron-bombardment ion source," NASA TN D-585 (January 1960).

[5] Thoneman, P. C., "A high current proton source," AERE GP/R1190 (1958).

[6] Kistemaker, J. and Harrison, E. R., "On ion sources with high efficiency and intensity," Nucl. Instr. Methods **11**, 179–184 (1961).

[7] Brewer, G. R., "Formation of high-density electron beams," J. Appl. Phys. **28**, 7–15 (1957).

[8] Van Duzer, T., Buckey, C. R., and Brewer, G. R., "Trajectory tracer for charged particles which includes magnetic field and space charge," Rev. Sci. Instr. **34**, 558–567 (1963).

[9] Langmuir, I., "Positive ion currents in the positive column of mercury arc," Gen. Elec. Rev. **26**, 731–735 (1923).

[10] Child, C. D., "Discharge from hot CaO," Phys. Rev. **32**, 492–511 (1911).

[11] Langmuir, I. and Blodgett, K., "Currents limited by space charge between concentric spheres," Phys. Rev. **24**, 49–59 (1924).